

**Microstructural changes in acid milk gels due to temperature-controlled high-intensity ultrasound treatment
Quantification by analysis of super-resolution microscopy images**

James Glover, Zachary; Gregersen, Sandra Beyer; Wiking, Lars; Hammershøj, Marianne; Simonsen, Adam Cohen

Published in:
International Journal of Dairy Technology

DOI:
10.1111/1471-0307.12838

Publication date:
2022

Document version:
Accepted manuscript

Citation for polished version (APA):
James Glover, Z., Gregersen, S. B., Wiking, L., Hammershøj, M., & Simonsen, A. C. (2022). Microstructural changes in acid milk gels due to temperature-controlled high-intensity ultrasound treatment: Quantification by analysis of super-resolution microscopy images. *International Journal of Dairy Technology*, 75(2), 321-328. <https://doi.org/10.1111/1471-0307.12838>

Go to publication entry in University of Southern Denmark's Research Portal

Terms of use

This work is brought to you by the University of Southern Denmark.
Unless otherwise specified it has been shared according to the terms for self-archiving.
If no other license is stated, these terms apply:

- You may download this work for personal use only.
- You may not further distribute the material or use it for any profit-making activity or commercial gain
- You may freely distribute the URL identifying this open access version

If you believe that this document breaches copyright please contact us providing details and we will investigate your claim.
Please direct all enquiries to puresupport@bib.sdu.dk

1
2
3
4
5
6
7
8
9
10
11
12
13
14
15
16
17
18
19
20
21
22
23
24
25
26
27

DR SANDRA GREGERSEN (Orcid ID : 0000-0001-9601-317X)

Article type : Research Article

Microstructural changes in acid milk gels due to temperature controlled high-intensity ultrasound treatment: Quantification by analysis of super-resolution microscopy images

Glover Z J.^a, Gregersen S B.^{b*}, Wiking L.^b, Hammershøj M^b, Simonsen A C^a

^a Department of Physics, Chemistry and Pharmacy, University of Southern Denmark, Campusvej 55, 5230 Odense M, Denmark.

^b Department of Food Science, Aarhus University, Agro Food Park 48, 8200 Aarhus N, Denmark.

* Corresponding Author.

Running Title: HIU milk gel super-res image analysis

Abstract

High Intensity Ultrasound (HIU) can be applied to food materials to create novel structures and textures, and as a method of processing. HIU treatment of milk modifies the gelation behaviour, but the microstructural impact is poorly understood. Milk samples were treated with HIU at three temperatures; 27°C, 50°C, and 70°C. Acid milk gels were formed from the milks and imaged using Super-resolution Stimulated Emission Depletion (STED) and confocal microscopy. Quantitative image analysis was applied and demonstrated that HIU treatment lead to measurable changes in both protein network morphology and degree of association of the fat droplets with the protein network.

Keywords

Super-resolution microscopy, Stimulated Emission Depletion (STED) microscopy, Quantitative image analysis, High intensity ultrasound, milk acid gel microstructure.

This is the author manuscript accepted for publication and has undergone full peer review but has not been through the copyediting, typesetting, pagination and proofreading process, which may lead to differences between this version and the [Version of Record](#). Please cite this article as [doi: 10.1111/1471-0307.12838](https://doi.org/10.1111/1471-0307.12838)

This article is protected by copyright. All rights reserved

28

29

30

31 **Introduction**

32 Emerging alternatives to traditional processes are being explored within the food industry. High Intensity Ultrasound (HIU)
33 treatments are an example of alternative processes that are capable of modifying the functionality and behaviour of materials
34 (Watson *et al.* 2013), including foods (Awad *et al.* 2012; Povey 2017), which can produce altered functionalities conferring specific
35 benefits to the manufacturer. High power ultrasound pre-treatment of milk has been explored in recent years and has been shown
36 to lead to changes in the gel strength of acid milk gels (Gregersen Wiking and Hammershøj, 2019; Nguyen and Anema, 2010;
37 2017) and can improve yoghurt texture (Riener *et al.* 2009). An understanding of the effects of HIU treatment on gel
38 microstructure at a spatial resolution related to physical and chemical properties is lacking.

39 Ultrasound is defined as sound waves with a frequency above the human audible range (20 kHz). There are two broad classes of
40 ultrasound that may be utilised in food and dairy product structures, low intensity ultrasound ($< 1 \text{ W/cm}^2$) can be utilised to
41 measure and characterise materials as it is non-destructive, whereas HIU refers to an intensity range that will lead to cavitation
42 and material modification ($>1 \text{ W/cm}^2$) (Awad *et al.* 2012). HIU leads to material modification through several processes;
43 fluctuations in pressure lead to the formation of bubbles, the size of which is related to the acoustic frequency. Bubbles move
44 through the fluid due to the acoustic field and though the process of rectified diffusion grow until they reach a certain size at which
45 point they collapse. Bubble collapse produces locally high temperatures and turbulence (Kentish and Fang 2014). The turbulence
46 generated from HIU treatment has a homogenising effect in food and dairy systems, which can result in functional and structural
47 changes and can be exploited by manufactures which has been reviewed recently (Carrillo-Lopez *et al.* 2021).

48 When considering structured dairy products the major macro components of interest are proteins and fat. Milk fat is present in the
49 form of milk fat droplets, predominantly composed of triglycerides, with a surrounding phospholipid stabilising layer; the Milk Fat
50 Globule Membrane (MFGM). The MFGM contains an array of complex proteinaceous and glycosylated components and provides
51 stability to the milk fat globules (Huppertz and Kelly 2006). Milk proteins can be split into the caseins, which are insoluble at pH
52 4.6, with the remainder being the whey proteins (20%). Caseins are present in the form of casein micelles, which are a complex
53 supramolecular assembly of four monomeric subunits held together through hydrogen bonding, hydrophobic interactions and ionic
54 interactions mediated through calcium phosphate nanoclusters (De Kruif *et al.* 2012). Casein micelle aggregation can be induced
55 through acidification to overcome the net negative surface charge present on the micelles or by chymosin cleavage of the
56 electronegative region of κ -casein, present at the micelle surface and contributes to steric and electronegative stability to the
57 micelles. The whey proteins are soluble, globular proteins and the dominant whey protein in bovine milk is β -lactoglobulin, which
58 when denatured exposes a free reactive thiol group which can lead to protein-protein disulphide bond interactions (Kethireddipalli

59 Hill and Dalgleish 2011; Chatterton *et al.* 2006). Under shear homogenisation the milk fat droplets are broken apart into more,
60 smaller droplets. Smaller fat droplets have an increased surface area in relation to the volume, hence, the native MFGM is not
61 sufficient to cover this newly exposed surface. Casein and whey proteins associate with the fat globule surface as they are
62 amphipathic and lower the total surface energy. Homogenising therefore effectively functionalise the surface of fat droplets with
63 molecules that can participate in further protein-protein interactions and network formation (Cho Lucey and Singh 1999).
64 Processes that can affect the degree of whey protein denaturation and fat droplet composition have potential to fine tune the
65 functional behaviour of milk for different applications.

66 HIU treatment has been demonstrated to lead to microstructural changes in various protein gel systems. HIU has been shown to
67 improve gel properties of porcine myosin by reducing aggregate size and increasing solubility (Sun *et al.* 2021) and to modify the
68 properties of α -lactalbumin (Qayum *et al.* 2021) and surimi (Gao *et al.* 2021; Liang *et al.* 2020) leading to increased water holding
69 capacity and altered gel morphology (Liang *et al.* 2020). The strength of rennet induced goat milk gels has also been shown to
70 increase following HIU treatment, due to protein structure modifications and changes in gel morphology (Ragab *et al.* 2020). The
71 combination of HIU and heat have been demonstrated affect gel strength and water holding in soy protein isolate (Zhao *et al.*
72 2021). In dairy products, HIU treatment can lead to whey protein denaturation below the denaturation temperature of whey protein
73 (Gregersen *et al.* 2019; Shanmugam, Chandrapala and Ashokkumar 2012; Villamiel and de Jong 2000). HIU induced
74 homogenisation of milk fat globules leading to changes in the MFGM protein composition (Gregersen *et al.* 2019) and has been
75 shown to retain more of the MFGM proteins compared to traditional homogenisation (Liu *et al.* 2021). Furthermore, the intensity of
76 HIU treatment leads to modification in protein-protein and protein-lipid interactions (Bui *et al.* 2021), which is likely to have an
77 effect on how the protein and lipid components form structure.

78 Whilst HIU treatments have been demonstrated to alter the interaction between protein and fat in dairy samples, the subsequent
79 impact upon gel microstructure has not been visualised or quantified to date. In food science, the ability to draw a causal link
80 between a material's microstructure and its emergent physical and chemical properties remains elusive (Aguilera, Stanley and
81 Baker 2000). Through the application of high-resolution microscopy and complementary image analysis methods, the effects of
82 alternative processing methods can be quantified allowing comparison to known physical and chemical changes, providing a more
83 complete map of interactions at different length scales.

84 Stimulated Emission Depletion (STED) microscopy is a super-resolution technique (Hell and Wichmann 1994; Hell 2007) that has
85 recently been applied to the imaging of dairy product structures but remains under-exploited in the imaging of food systems
86 (Glover and Holmes 2020; Glover *et al.* 2020). The advantage of STED in imaging colloidal structures is that the only perturbation
87 required is the addition of a fluorescent dye. Samples do not have to be fixed or dried, minimising the potential for structural
88 artefacts as well as reducing analysis time (Glover *et al.* 2019a).

89 Quantitative image analysis is required to extract the full level of detail contained within super-resolution images. Methods based
90 on autocorrelation analysis have been used to quantify structures in various food materials (Ako *et al.* 2009; Urbonaite *et al.* 2016;

91 Ersch *et al.* 2016; Urbonaite *et al.* 2015; Ainis *et al.* 2019). Recent developments have allowed quantification of the microstructure
92 of milk acid gels (Glover, *et al.* 2019a; Glover *et al.* 2019b; Gregersen *et al.* 2021). A combination of autocorrelation and cross-
93 correlation analyses have been presented to quantify the protein network and the spatial relationship between protein and fat in
94 two component Pickering stabilised emulsions and dairy gels (Araiza-Calahorra *et al.* 2020; Glover *et al.* 2019b). Quantification
95 aids the understanding of how molecular changes during HIU treatment affect the structuring following treatment, and how that
96 leads to changes in macroscopic properties. It has been shown recently that relevant parameters extracted from microstructural
97 quantification relate to the macroscopic behaviour of a gel system for milk samples treated with hydrodynamic cavitation and
98 pressure homogenisation (Gregersen *et al.* 2021).

99 The aim of this study was to be able to understand the microstructural changes that occur during temperature controlled high
100 intensity ultrasound treatment. Two temperatures below denaturation temperature of whey protein were used, where whey protein
101 denaturation has been shown to occur due to HIU (Gregersen *et al.* 2019). A temperature of 70 °C where both thermal and HIU
102 effects can lead to whey protein denaturation and structural modification. Microstructural changes were quantified through image
103 analysis of STED microscopy images. The output from the image analysis was compared to measurements of the casein micelle
104 size and discussed in relation to previously acquired macroscopic data.

105

106 **Materials and Methods**

107 Milk samples were obtained and treated as per (Gregersen *et al.* 2019), a brief description follows.

108 **Materials**

109 Commercial full fat (3.5% fat), pasteurised (72 °C, 15 s), un-homogenised milk was obtained from a local store at maximum 2
110 days after processing at the dairy and stored at 5 °C. 1L packaged milk samples were pooled from which subsamples were taken.
111 Samples were analysed for protein, fat and dry matter content by a Milkoscan unit (Foss, Hillerød, Denmark), which showed an
112 average milk composition in g/L of; 35.4 ± 0.05 , 35.2 ± 0.07 and 126.2 ± 0.86 for protein, fat and dry matter, respectively.

113 **Ultrasound treatment**

114 Milk was subjected to ultrasound treatment in a 100 mL ultrasonic flow cell (Sonolab SL10 ultrasonic, Syrris Ltd, United Kingdom)
115 operating at 20 kHz. Milk samples were heated to three treatment temperatures (27 °C, 50 °C and 70 °C) using a water bath, and
116 ultrasonication was performed at 30 W with an estimated field energy intensity in the flow cell of 273W/L. These parameters were
117 selected to be able to investigate the microstructure in samples where other physical and chemical parameters have been
118 described (Gregersen *et al.* 2019). A total treatment volume of 800 mL milk was circulated in the flow cell system at 200 mL/min
119 (Watson-Marlow 520DU peristaltic pump, United Kingdom) from a jacketed glass reactor (2000 mL) with circulating water for
120 temperature control. During treatment, mixing was ensured with a magnetic stirrer at 200 rpm (IKA RCT basic IKAMAG®)

121 magnetic stirrer, IKA®-Werke GmbH & Co. KG, Germany). The total treatment time was 30 min, given an average residence time
122 in the flow cell of 4.13 min. Samples were prepared in duplicate.

123 **Sample Preparation**

124 Milk fat was stained for imaging with Nile Red (Sigma Aldrich, UK) to a concentration of 2.5 μM in the milk. Stained samples were
125 left overnight at 5°C. Milk acid gels were prepared by adding 0.25 g of Glucono- δ -Lactone (GDL)(Sigma-Aldrich, USA) to 10 mL of
126 the pre-stained milk giving a concentration of 2.5% GDL in the milk. The 10 mL of milk with GDL was inverted by hand for 1 min,
127 and 600 μL of milk was sampled to which 3 μL of Atto 488 NHS-Ester (Atto-Tec GmbH, Siegen, Germany), dissolved in DMSO
128 (99.9% pure, Sigma-Aldrich) was added to give a concentration of 510 μM in the milk. This volume was then transferred to a μ -
129 Slide 8 Well chamber (ibidi, Germany), and incubated at 35 °C for 90 min. Five gels were produced per milk sample, giving 10
130 gels per treatment, as milk samples were prepared in duplicate.

131 **Imaging Protocol**

132 Imaging was performed using a Leica TSC SP8 STED microscope (Leica GmbH, Mannheim, Germany). Images were taken with
133 two sequential channels; first with excitation using an incident laser at 560 nm with detection between 570 and 700 nm, second
134 with excitation at 480 nm and detection between 490 and 550 nm with STED depletion at 592 nm. The fat droplets were imaged
135 with confocal resolution as the microscope was equipped for single channel STED imaging, the protein network was imaged with
136 STED resolution. Both setups utilised a pulsed white light laser and gated hybrid detector (0.3 - 6 ns). The pixel size 34 nm using
137 a zoom of 2.5X, acquiring images of 1384 x 1384 pixels equal to 46.5 μm^2 using a HCX PL AP 100X/1.40 OIL STED objective. A
138 minimum of 10 images were taken per gel, i.e. a total of 100 images per sample type. Images were taken $>5 \mu\text{m}$ above the glass
139 interface to avoid boundary effects. The suitability of these sample preparation methods has been shown by Glover *et al.* (2019a).

140 **Quantitative Image Analysis**

141 Image analysis was conducted with MATLAB R2018b (Mathworks, U.S.A.) as described by Glover *et al.* (2019a; 2019b) using
142 auto- and cross-correlation-based methods. The parameters extracted from the image analysis are: ξ_p (μm), the typical length
143 scale of the protein domains in the protein channel image, λ (μm), the inter-pore distance in the protein channel image, D_f (-), the
144 fractal dimension in the protein channel image, ξ_f (μm), the typical size of the fat droplets in the fat channel image and Λ (μm), the
145 typical distance from the fat droplet interface to the centre of mass of the neighbouring protein domain determined between the fat
146 and protein channels.

147 One-way Analysis of Variance (ANOVA) with treatment temperature as class variable and with post-hoc Tukey's honestly
148 significant difference tests at minimum 95 %-level ($P \leq 0.05$) were conducted on the data extracted from the image analysis.

149 **Casein Micelle Size**

150 Skim milk was obtained by centrifugation at $2643 \times g$ for 30 min at 4°C , and diluted 1:10 with simulated milk ultra-filtrate buffer
151 (SMUF), prepared according to Jenness and Koops (1962). The average casein micelle size (Volume based) was determined by
152 dynamic light scattering using a NANO-flex particle size analyzer (Microtrac Inc., Montgomeryville, PA, USA).

153

154 Results and Discussion

155 Figure 1 shows representative super-resolution STED images of the acid milk gel samples upon which quantitative analysis was
156 performed. Figure 2 shows the outcome from the image analysis of the four gels samples, and Table 1 shows casein micelle size
157 against the output parameters from the image analysis. It is optimal to compare changes in distributions of image analysis
158 parameters, but the mean and standard deviations are included in Table 1 for statistical comparison.

159 The mean casein micelle size showed a trend to increase from the untreated control to the HIU treated samples, which was
160 significantly highest at 70°C , (Table 1). A temperature of 70°C will lead to denaturation of whey protein, and therefore higher
161 temperatures during HIU treatments leads to increased denaturation of whey protein. HIU treatment below the denaturation
162 temperature of the whey proteins does still lead to whey protein denaturation as previously shown (Gregersen et al. 2019) and
163 therefore the treatment of 70°C shows the combined effects of thermal and HIU treatment. When β -lactoglobulin denatures, a
164 free thiol-group is exposed, which can covalently bind to both free thiol groups on the κ -casein molecules, situated on the surface
165 of the casein micelles (Steffl *et al.* 1999; Lucey, Munro and Singh 1999).

166 The modification in casein micelle size with HIU treatment at high temperature was accompanied by a thinner gel structure, shown
167 by the size of the typical length scale in the images, ξ_p , which corroborates with previous observations, where smaller ξ_p values
168 also correlated to gels with a higher G' (Gregersen *et al.* 2021). Thus, a higher degree of denatured whey protein effectively
169 increased micelle size, and modified the behaviour of the aggregating micelles and altered the gel structures, which was
170 quantified here. It has previously been shown that higher levels of denatured whey protein relate to firmer gels being formed as
171 there are more protein-protein interactions in the gel network (Anema and Li, 2000; 2003; Glover *et al.* 2020; Gregersen *et al.*
172 2021). It is a counter-intuitive observation that the size of the aggregating particles increases, but the typical size of the
173 aggregated structures decreases. If the same quantity of protein is arranged to have thinner structures, there will be an increase in
174 the protein network's surface area, which leads to increased moisture binding and increased gel strength (Glover *et al.* 2020).
175 Increased moisture binding in protein gels following HIU treatment has been documented in several other materials such as surimi
176 (Liang *et al.* 2020) and soy protein isolate (Zhao *et al.* 2021). STED microscopy and the image analysis applied here allows for the
177 detection and quantification at a significant level, allowing gels produced from milks with different processing histories to be
178 differentiated from each other. The combination of the interpore distance and fractal dimension can significantly differentiate
179 between the four gel samples prepared, highlighting the fact that one single parameter is not sufficient to capture the subtle
180 differences in gel structure and morphology. It can be seen in figure 2 that there is a trend in λ , the typical long order repeat
181 distance in the images, which represents the interpore distance, where the control sample has the largest λ values. HIU treatment

182 leads to a reduction in the inter-pore distance which decreases with increasing temperature of treatment. When considered
183 alongside ξ_p , the reduction in both structure size and interpore distance indicates a structure with more pores and a thinner
184 continuous protein phase. The fractal dimension can be interpreted as showing how ragged the gel interface and to what extent
185 the network completely fills a space (Glover *et al.* 2019). Figure 2c shows that the network in the control sample is the most
186 space filling, supporting the interpretation that HIU treatment leads to morphological changes of thinner structures and increased
187 porosity which are less space filling.

188 The fat droplet radius, ξ_f , decreased from the untreated control to HIU treatment at 50 °C and 70 °C, and also show a narrowing in
189 the distribution with HIU treatment compared to the control sample. ξ_f is a measure of the average size of the fat droplets within
190 the microscopy image and is not equivalent to a complete particle size distribution. The parameter, Λ , which relates to the typical
191 distance from a fat droplet interface to the centre of mass of a neighbouring protein domain shows the largest difference between
192 the control sample and the HIU treated samples. The fat droplets in the HIU treated samples are more closely embedded in the
193 protein matrix. Following a size reduction, milk proteins will adsorb to the newly exposed fat droplet surface and HIU treatment is
194 shown to provide a shift in protein associated with the MFGM (Gregersen *et al.* 2019). Hansen *et al.* (2020) showed that whey
195 protein association to the milk fat globule membrane is not only mediated through di-sulphide bond formation and occurs through
196 other intermolecular interactions such as hydrophobic interactions. Protein adsorption effectively functionalises the fat droplets to
197 be able to become an active filler in the protein network increasing the gel strength (Van Vliet 1988), which has been observed in
198 acid milk gels (Gregersen *et al.* 2021). The image analysis used here can measure the degree to which the fat droplets become
199 more deeply incorporated into the protein network. The distances determined are below the diffraction limit of light and could
200 therefore only be measured using a super-resolution technique.

201 The effects of whey protein denaturation on the structure, rheological properties and water binding capacities of conventionally
202 processed dairy products are well studied (Cho *et al.* 1999; Van Vliet 1988). The results shown in this study highlight the fact that
203 the structural changes are temperature dependent and therefore the degree of modification introduced by HIU treatment could be
204 modulated through temperature control. When considering the fate of industrially produced dairy gels there are two broad
205 possibilities. Firstly, where a high level of whey protein denaturation is beneficial in order to have more protein participate in the
206 network, increase yield and water holding, improving the texture and minimising syneresis as typical with yoghurts and similar
207 fermented dairy products (Lopez Camier and Gassi, 2007). Alternatively in gels produced in a cheese vat the level of denatured
208 whey proteins needs to be controlled, partially because increased levels of whey protein confer bitter flavours to matured cheeses
209 and also because whey proteins extracted from the liquid whey are much more valuable economically compared to being in the
210 cheese matrix (Yadav *et al.* 2015). The results from the microstructural analysis suggested that it may be possible to use HIU
211 treatments at lower temperatures for a homogenising effect, leading to a reduction in milk fat globule size and association of the
212 fat droplets and protein network, without incurring higher levels of protein denaturation, supported by the less drastic change in
213 micelle size measured here and corroborated by the study of Gregersen *et al.* (2019). Therefore, temperature control during
214 treatment could allow a cheese maker to optimise the homogenisation process to maximise the entrapment of fat and boost yield,

215 whilst minimising whey protein losses, therefore maximising the potential of all the milk components. This study utilised
216 pasteurised milk and therefore already contained some quantity of denatured whey protein and potential changes in the milk fat
217 globules prior to treatment. HIU treatment of raw milk could potentially have even more pronounced effects in modifying structure,
218 as the whey proteins will be denatured at the same time as the fat droplets are homogenised, thereby increasing the likelihood of
219 protein-fat interactions, which is worth future consideration.

220 The results presented here demonstrate the effects that HIU pre-treatment has on the microstructure of dairy acid gels in terms of
221 modification of the protein network, the homogenising effect HIU treatment has on the fat droplets and the subsequent interactions
222 between the fat droplets and protein matrix. Whilst several studies have measured the various physical and chemical changes that
223 occur during HIU treatment, this is the first demonstration with quantitative measures showing that the gel microstructure is
224 significantly altered. The combined method of super-resolution imaging and quantitative image analysis have demonstrated value
225 in being able to assess and differentiate samples prepared with emerging, alternative techniques. The use of quantitative imaging
226 methodologies will be required to reach a stage where causal links can be drawn between microstructure and the emergent
227 physical behaviours such as rheology, water holding or consumer acceptance.

228

229 **Conclusions**

230 A combination of super-resolution STED microscopy and correlation-based image analysis techniques quantified differences in
231 the microstructure of acid gels from untreated and HIU treated milk. HIU treatments at 27 and 50 °C showed the effects of high
232 intensity ultrasound on the sample, whereas the changes shown at 70 °C illustrate the combined effect of thermal denaturation
233 and HIU treatment. Results demonstrate how HIU, at all temperatures tested, leads to formation a finer gel structures, shown by
234 the size of the typical length scale in the images, ξ_p . HIU treatment also provide a closer association of the fat globules with the
235 protein network, quantified in terms of a reduction in parameter, Λ , which relates to the typical distance from a fat droplet interface
236 to the centre of mass of a neighbouring protein domain shows the largest difference between the control sample and the HIU
237 treated samples. The quantified differences in structure are of importance for understanding HIU induced changes in the acid gel
238 formation of milk.

239 **Conflict of Interests**

240 The authors have no competing interests.

241 **Acknowledgements**

242 The authors acknowledge the Danish Molecular Biomedical Imaging Center (DaMBIC, University of Southern Denmark) for the
243 use of the bioimaging facilities

244 **Funding**

245 This work was funded by The Danish Dairy Research Fund, Arla Foods amba, Arla Foods Ingredients P/S, Aarhus University and
246 University of Southern Denmark

247 **Data Availability Statement**

248 Research data are not shared

249 **References**

250 Aguilera J M Stanley D W and Baker K W (2000) New dimensions in microstructure of food products. *Trends in Food Science &*
251 *Technology* **11** 3-9.

252 Ainis W N Ersch C Farinet C Yang Q Glover Z J and Ipsen R (2019) Rheological and water holding alterations in mixed gels
253 prepared from whey proteins and rapeseed proteins. *Food Hydrocolloids* **87** 723-733.

254 Ako K Durand D Nicolai T and Becu L (2009) Quantitative analysis of confocal laser scanning microscopy images of heat-set
255 globular protein gels. *Food Hydrocolloids* **23** 1111-1119.

256 Anema S G and Li Y (2000) Further studies on the heat-induced pH-dependent dissociation of casein from the micelles in
257 reconstituted skim milk LWT. *Food Science and Technology* **33** 335-343.

258 Anema S G and Li Y (2003) Association of denatured whey proteins with casein micelles in heated reconstituted skim milk and its
259 effect on casein micelle size. *Journal of dairy Research* **70** 73-83.

260 Araiza-Calahorra A Glover Z J Akhtar M and Sarkar A (2020) Conjugate microgel-stabilized Pickering emulsions: Role in delaying
261 gastric digestion. *Food Hydrocolloids* 105794.

262 Awad T S Moharram H A Shaltout O E Asker D Y M M and Youssef M M (2012) Applications of ultrasound in analysis processing
263 and quality control of food: A review. *Food research international* **48** 410-427.

264 Bui A T H Cozzolino D Zisu B and Chandrapala J (2021) Infrared analysis of ultrasound treated milk systems with different levels
265 of caseins whey proteins and fat. *International Dairy Journal*. **117** 104983.

266 Carrillo-Lopez L M Garcia-Galicia I A Tirado-Gallegos J M Sanchez-Vega R Huerta-Jimenez M Ashokkumar M and Alarcon-Rojo
267 A D (2021) Recent advances in the application of ultrasound in dairy products: Effect on functional physical chemical
268 microbiological and sensory properties. *Ultrasonics Sonochemistry* 105467.

269 Chatterton D E Smithers G Roupas P and Brodkorb A (2006) Bioactivity of β -lactoglobulin and α -lactalbumin—Technological
270 implications for processing. *International Dairy Journal* **16** 1229-1240.

271 Cho Y H Lucey J A and Singh H (1999) Rheological properties of acid milk gels as affected by the nature of the fat globule surface
272 material and heat treatment of milk. *International Dairy Journal* **9** 537-545.

273 De Kruif C G Huppertz T Urban V S and Petukhov A V (2012) Casein micelles and their internal structure. *Advances in colloid and*
274 *interface science* **171** 36-52.

275 Ersch C Meinders M B Bouwman W G Nieuwland M van der Linden E Venema P and Martin A H (2016) Microstructure and
276 rheology of globular protein gels in the presence of gelatin. *Food Hydrocolloids* **55** 34-46.

277 Gao X Yongsawatdigul J Wu R You J Xiong S Du H and Liu R (2021) Effect of ultrasound pre-treatment modes on gelation
278 properties of silver carp surimi. *LWT* **150** 111945.

279 Glover Z J & Holmes M J (2020) Physics in the rehydration and structure formation of recombined dairy products. In Povey M J
280 *Physics in Food Manufacturing: case studies in fundamental and applied research* IOP Publishing.

281 Glover Z J Bisgaard A H Andersen U Povey M J Brewer J R and Simonsen A C (2019b) Cross-correlation analysis to quantify
282 relative spatial distributions of fat and protein in super-resolution microscopy images of dairy gels. *Food Hydrocolloids* **97** 105225.

283 Glover Z J Ersch C Andersen U Holmes M J Povey M J Brewer J R and Simonsen A C (2019a) Super-resolution microscopy and
284 empirically validated autocorrelation image analysis discriminates microstructures of dairy derived gels. *Food hydrocolloids* **90** 62-
285 71.

286 Glover Z J Francis M J Bisgaard A H Andersen U Johansen L B Povey M J Holmes M J Brewer J R and Simonsen A C (2020)
287 Dynamic moisture loss explored through quantitative super-resolution microscopy spatial micro-viscosity and macroscopic
288 analyses in acid milk gels. *Food Hydrocolloids* **101** 105501.

289 Gregersen S B Glover Z J Wiking L Simonsen A C Bertelsen K Pedersen B Poulsen K R Andersen U and Hammershøj M (2021)
290 Microstructure and rheology of acid milk gels and stirred yoghurts—quantification of process-induced changes by auto-and cross
291 correlation image analysis. *Food Hydrocolloids* **111** 106269.

292 Gregersen S B Wiking L and Hammershøj M (2019) Acceleration of acid gel formation by high intensity ultrasound is linked to
293 whey protein denaturation and formation of functional milk fat globule-protein complexes. *Journal of Food Engineering* **254** 17-24.

294 Hansen S F Nielsen S D Rasmusen J T Larsen L B and Wiking L (2020) Disulfide bond formation is not crucial for the heat-
295 induced interaction between β -lactoglobulin and milk fat globule membrane proteins. *Journal of Dairy Science* **03** 5874-5881.

296 Hell S W (2007) Far-field optical nanoscopy. *science* **316** 1153-1158.

297 Hell S W and Wichmann J (1994) Breaking the diffraction resolution limit by stimulated emission: stimulated-emission-depletion
298 fluorescence microscopy. *Optics letters* **19** 780-782.

299 Huppertz T and Kelly A L (2006) Physical chemistry of milk fat globules. *Advanced dairy chemistry volume 2 lipids* 173-212
300 Springer Boston MA.

- 301 Jenness R and Koops J (1962) Preparation and properties of a salt solution which simulates milk ultrafiltrate. *Netherlands Milk*
302 *and Dairy Journal* **16** 153-164.
- 303 Kentish S and Feng H (2014) Applications of power ultrasound in food processing. *Annual review of food science and technology*
304 **5** 263-284.
- 305 Kethireddipalli P Hill A R and Dalgleish D G (2011) Interaction between casein micelles and whey protein/ κ -casein complexes
306 during renneting of heat-treated reconstituted skim milk powder and casein micelle/serum mixtures. *Journal of agricultural and*
307 *food chemistry* **59** 1442-1448.
- 308 Liang F Zhu Y Ye T Jiang S Lin L and Lu J (2020) Effect of ultrasound assisted treatment and microwave combined with water
309 bath heating on gel properties of surimi-crabmeat mixed gels. *LWT* **133** 110098.
- 310 Liu Y Boeren S Zhang L Zhou P and Hettinga K (2021) Ultrasonication retains more milk fat globule membrane proteins compared
311 to equivalent shear-homogenization. *Innovative Food Science & Emerging Technologies* **70** 102703.
- 312 Lopez C Camier B and Gassi J Y (2007) Development of the milk fat microstructure during the manufacture and ripening of
313 Emmental cheese observed by confocal laser scanning microscopy. *International Dairy Journal* **17** 235-247.
- 314 Lucey J A Munro P A and Singh H (1999) Effects of heat treatment and whey protein addition on the rheological properties and
315 structure of acid skim milk gels. *International Dairy Journal* **9** 275-279.
- 316 Nguyen N H & Anema S G (2010) Effect of ultrasonication on the properties of skim milk used in the formation of acid gels.
317 *Innovative Food Science & Emerging Technologies* **11** 616-622.
- 318 Nguyen N H & Anema S G (2017) Ultrasonication of reconstituted whole milk and its effect on acid gelation. *Food chemistry* **217**
319 593-601.
- 320 Povey M J (2013) Ultrasound particle sizing: A review. *Particuology* **11** 135-147.
- 321 Povey M J (2017) Applications of ultrasonics in food science-novel control of fat crystallization and structuring. *Current Opinion in*
322 *Colloid & Interface Science* **28** 1-6.
- 323 Qayum A Hussai M Li M Li J Shi R Li T Anwar A Ahmed Z Hou J and Jiang Z (2021) Gelling, microstructure and water-holding
324 properties of alpha-lactalbumin emulsion gel: Impact of combined ultrasound pretreatment and laccase cross-linking. *Food*
325 *Hydrocolloids* **110** 106122.
- 326 Ragab E S Zhang S Pang X Lu J Nassar K S Yang B Obaroakpo U J and Lv J (2020) Ultrasound improves the rheological
327 properties and microstructure of rennet-induced gel from goat milk. *International Dairy Journal* **104** 104642.
- 328 Riener J Noci F Cronin D A Morgan D J & Lyng J G (2009) The effect of thermosonication of milk on selected physicochemical
329 and microstructural properties of yoghurt gels during fermentation. *Food Chemistry* **114** 905-911.

330 Shanmugam A Chandrapala J & Ashokkumar M (2012) The effect of ultrasound on the physical and functional properties of skim
331 milk. *Innovative Food Science & Emerging Technologies* **16** 251-258.

332 Steffl A Schreiber R Hafenmair M and Kessler H G (1999) Effect of denatured whey proteins on the rennet-induced aggregation of
333 casein micelles. *International dairy journal* **9** 401-402.

334 Sun Y Ma L Fu Y Dai H and Zhang Y (2021). The improvement of gel and physicochemical properties of porcine myosin under
335 low salt concentrations by pulsed ultrasound treatment and its mechanism. *Food Research International* **141** 110056.

336 Urbonaite V De Jongh H H J Van Der Linden E and Pouvreau L (2015) Water holding of soy protein gels is set by coarseness
337 modulated by calcium binding rather than gel stiffness. *Food hydrocolloids* **46** 103-111.

338 Urbonaite V Van der Kaaij S De Jongh H H J Scholten E Ako K Van der Linden E and Pouvreau L (2016) Relation between gel
339 stiffness and water holding for coarse and fine-stranded protein gels. *Food Hydrocolloids* **56** 334-343.

340 Van Vliet T (1988) Rheological properties of filled gels Influence of filler matrix interaction. *Colloid and Polymer Science* **266** 518-
341 524.

342 Villamiel M & de Jong P (2000) Influence of high-intensity ultrasound and heat treatment in continuous flow on fat proteins and
343 native enzymes of milk. *Journal of Agricultural and Food Chemistry* **48** 472-478.

344 Watson N J Johal R K Glover Z Reinwald Y White L J Ghaemmaghami A M Morgan S P Rose F R A J Povey M J W and Parker N
345 G (2013) Post-processing of polymer foam tissue scaffolds with high power ultrasound: a route to increased pore interconnectivity
346 pore size and fluid transport. *Materials Science and Engineering: C* **33** 4825-4832.

347 Yadav J S S Yan S Pilli S Kumar L Tyagi R D and Surampalli R Y (2015) Cheese whey: A potential resource to transform into
348 bioprotein functional/nutritional proteins and bioactive peptides. *Biotechnology Advances* **33** 756-774.

349 Zhao C Chu Z Miao Z Liu J Liu J Xu X Wu Y Qi B and Yan J (2021) Ultrasound heat treatment effects on structure and acid-
350 induced cold set gel properties of soybean protein isolate. *Food Bioscience* **39** 100827.

351

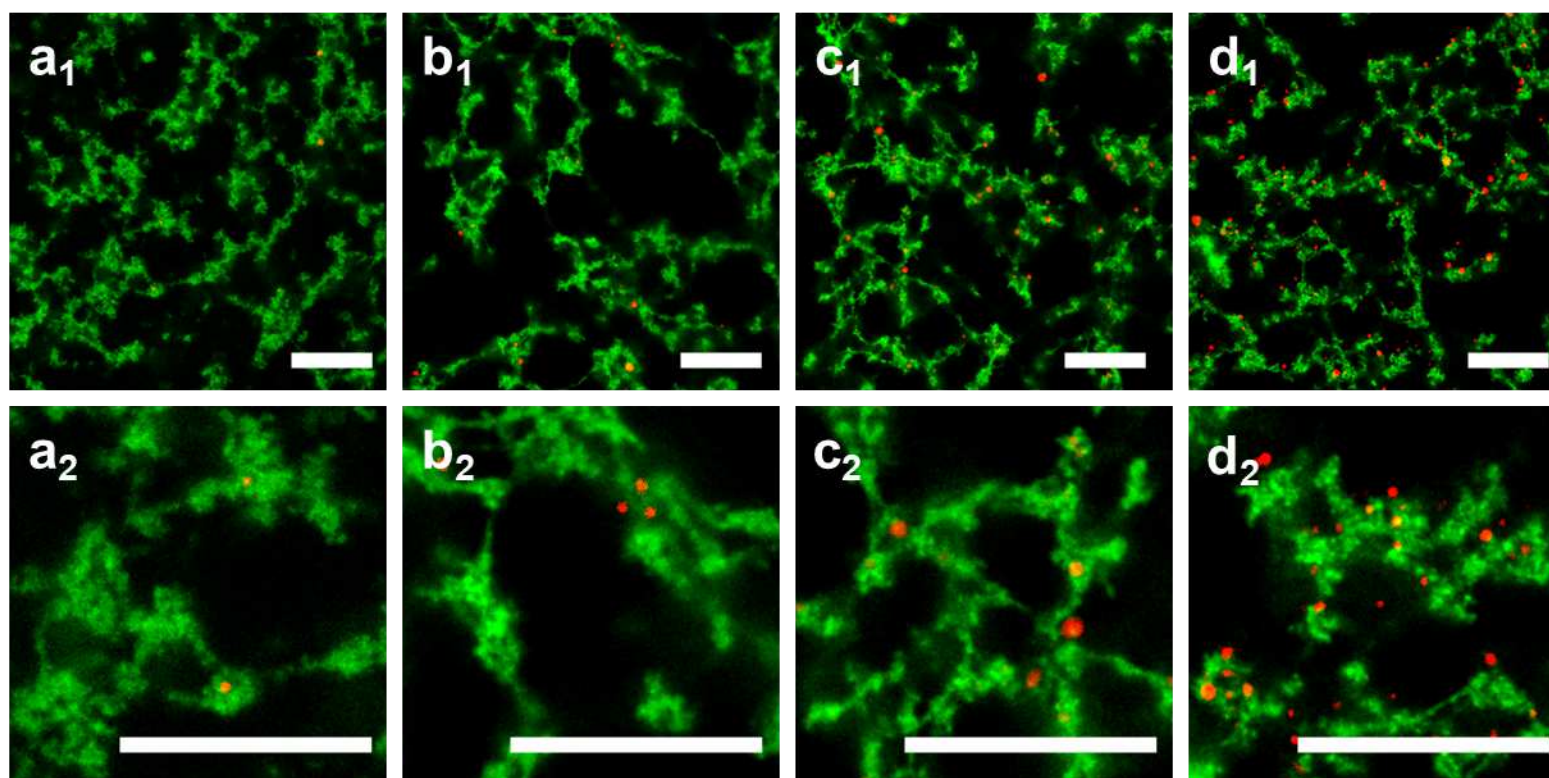
352

353

354

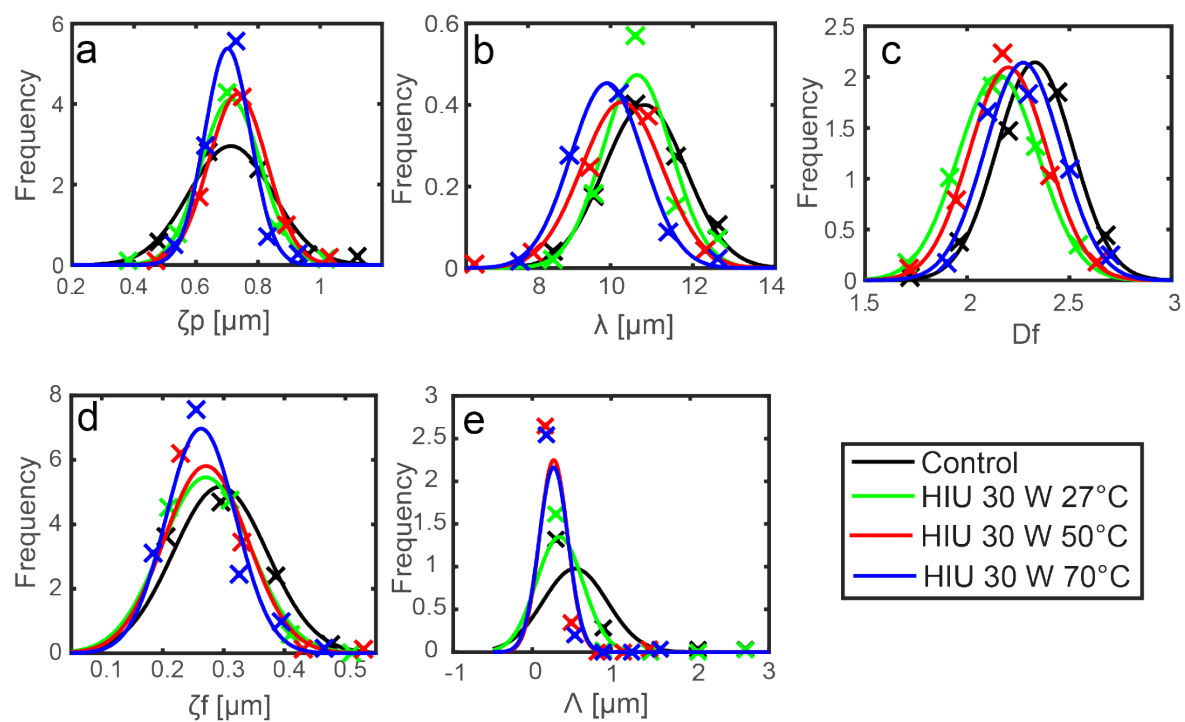
355

356 **Figures**



358

359 *Figure 1:* Typical two-colour Super-resolution Stimulated Emission Depletion (STED) and confocal microscopy images of acid milk gels with fat shown in the
 360 red channel (confocal) and the protein network shown in the green channel (STED). Acid gels were prepared from whole untreated milk control (a_1, a_2) and
 361 milk treated with high intensity ultrasound at 27°C (b_1, b_2), at 50°C (c_1, c_2) or at 70°C (d_1, d_2). Horizontal bar represents 10 μm .



362

363 *Figure 2:* Image analysis parameters extracted from microscopy images of acid milk gels prepared from whole untreated milk (control) or milk treating milk
 364 with high intensity ultrasound (HIU) at 27 °C, 50 °C or 70 °C. Typical length of the protein domain extracted from autocorrelation analysis (a). Average inter-
 365 pore distance in protein network from autocorrelation analysis (b). Fractal dimension determined from Fourier space analysis (c). The typical length scale of
 366 the fat droplets determined with autocorrelation analysis (d). Typical distance from fat droplet interface to centre of mass of neighbouring protein domain
 367 determined from cross-correlation analysis (e).

368

369

370

371

372

373

374

375

376 **Table**

377 Table 1: Effect of high intensity ultrasound treatment (HIU) of milk at different temperature on the casein micelle size and characteristic of the microstructure,
 378 by image analysis of microscopy images, in terms of the typical length scale of the protein domains (ξ_p), the inter-pore distance (λ), the fractal dimension in
 379 the protein channel (D_f), the typical size of the fat droplets (ξ_f) and the typical distance from the fat droplet interface to the centre of mass of the
 380 neighbouring protein domain (Λ). Lower case letters within each column denote significant differences between treatments ($P < 0.05$, $n=10$).

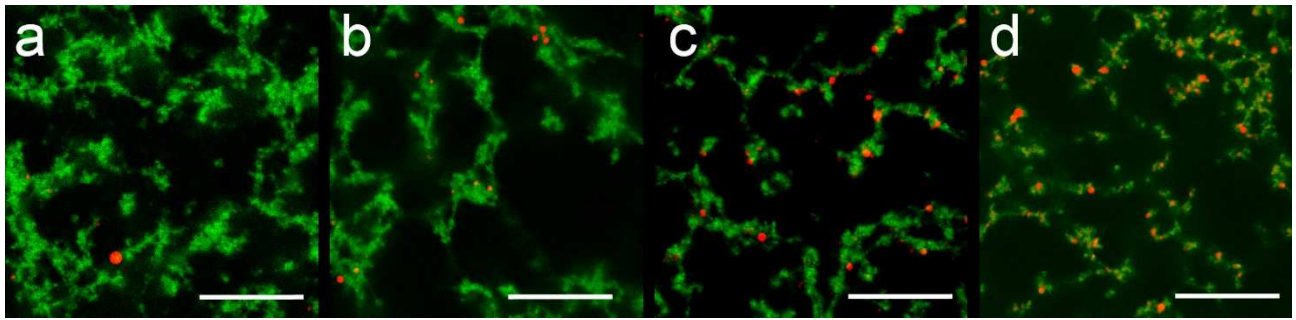
	Casein micelle size (μm)	ξ_p (μm)	λ (μm)	D_f (-)	ξ_f (μm)	Λ (μm)
No treatment	196.5 \pm 12.2 ^a	0.570 \pm 0.11 ^b	11.10 \pm 0.91 ^b	1.60 \pm 0.26 ^b	2.24 \pm 0.68 ^b	0.543 \pm 0.48 ^b
HIU 27 °C	221.6 \pm 18.0 ^{a, b}	0.546 \pm 0.10 ^{a, b}	10.77 \pm 0.96 ^{a, b}	1.60 \pm 0.37 ^{a, b}	2.23 \pm 0.51 ^{a, b}	0.346 \pm 0.30 ^a
HIU 50 °C	238.2 \pm 15.1 ^{a, b}	0.537 \pm 0.09 ^{a, b}	10.68 \pm 1.15 ^{a, b}	1.50 \pm 0.32 ^{a, b}	2.10 \pm 0.68 ^a	0.272 \pm 0.18 ^a
HIU 70 °C	277.8 \pm 16.5 ^b	0.477 \pm 0.07 ^a	10.65 \pm 1.00 ^a	1.49 \pm 0.29 ^a	1.98 \pm 0.30 ^a	0.271 \pm 0.18 ^a

381

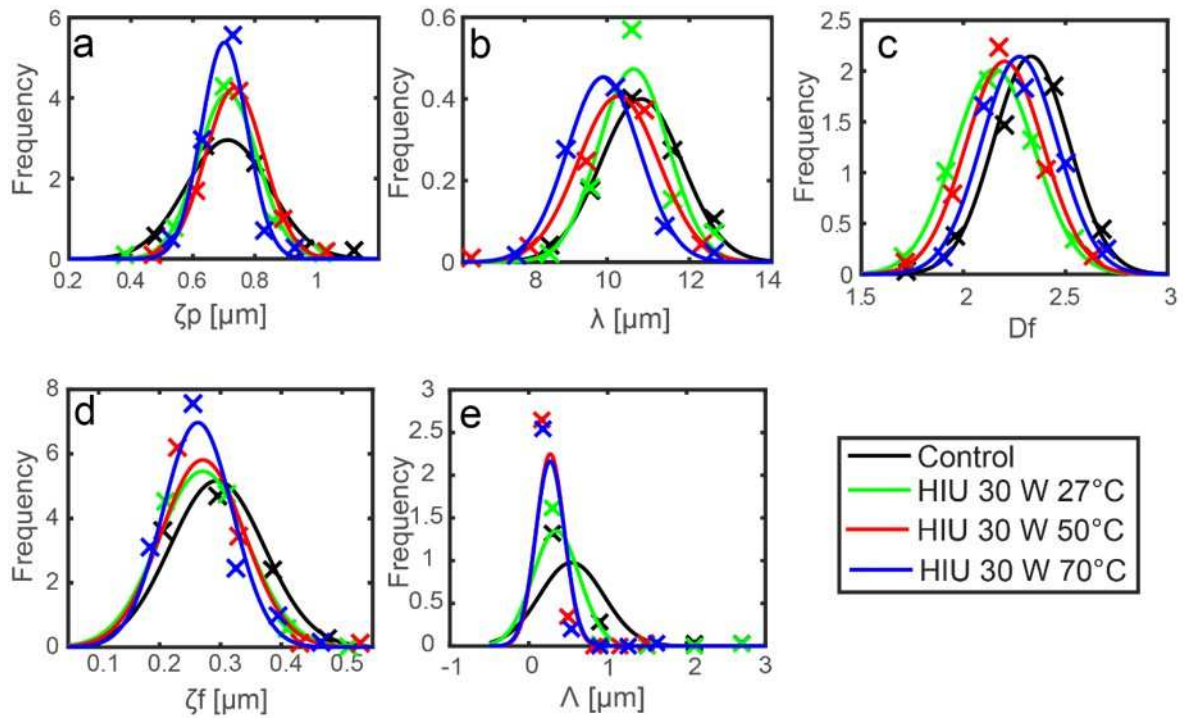
1 Table 1: Effect of high intensity ultrasound treatment (HIU) of milk at different temperature on the casein micelle size and characteristic of the microstructure,
 2 by image analysis of microscopy images, in terms of the typical length scale of the protein domains (ξ_p), the inter-pore distance (Λ), the fractal dimension in
 3 the protein channel (D_f), the typical size of the fat droplets (ξ_f) and the typical distance from the fat droplet interface to the centre of mass of the
 4 neighbouring protein domain (Λ). Lower case letters within each column denote significant differences between treatments ($P < 0.05$, $n=10$).

	Casein micelle size (μm)	ξ_p (μm)	Λ (μm)	D_f (-)	ξ_f (μm)	Λ (μm)
No treatment	196.5 ± 12.2^a	0.570 ± 0.11^b	11.10 ± 0.91^b	1.60 ± 0.26^b	2.24 ± 0.68^b	0.543 ± 0.48^b
HIU 27 °C	$221.6 \pm 18.0^{a,b}$	$0.546 \pm 0.10^{a,b}$	$10.77 \pm 0.96^{a,b}$	$1.60 \pm 0.37^{a,b}$	$2.23 \pm 0.51^{a,b}$	0.346 ± 0.30^a
HIU 50 °C	$238.2 \pm 15.1^{a,b}$	$0.537 \pm 0.09^{a,b}$	$10.68 \pm 1.15^{a,b}$	$1.50 \pm 0.32^{a,b}$	2.10 ± 0.68^a	0.272 ± 0.18^a
HIU 70 °C	277.8 ± 16.5^b	0.477 ± 0.07^a	10.65 ± 1.00^a	1.49 ± 0.29^a	1.98 ± 0.30^a	0.271 ± 0.18^a

5



idt_12838_f1.jpg



idt_12838_f2.jpg